Timing of formation of Beta Regio and its geodynamical implications

A. V. Vezolainen,[1] V. S. Solomatov,[1] J. W. Head,[2] A. T. Basilevsky,[3] and L.-N. Moresi[4]

Received 21 February 2002; revised 29 August 2002; accepted 5 September 2002; published 28 January 2003.

[1] Recent evidence suggests that the Beta Regio equatorial highland, generally considered to be a plume-related structure, was emplaced over a relatively short period of time in the recent Venus history (100–400 m.y.). We perform numerical simulations which use this evidence as a new constraint on geodynamic models and find that it is difficult to satisfy simultaneously the constraint on the uplift rate and the constraints on gravity, topography, and rheology. One possible solution is that the effective viscosity contrast between the mantle and the lithosphere does not exceed about 10^4. If our simple models do capture the basic dynamics of formation of Beta Regio, this value implies that the viscosity of the lithosphere is softer than olivine at subsolidus temperatures and that the Venusian lithosphere may not be much stronger than the terrestrial one. *INDEX TERMS:* 3210 Mathematical Geophysics: Modeling; 8147 Tectonophysics: Evolution of the Earth: Planetary interiors (5430, 5724); 6295 Planetology: Solar System Objects: Venus; 8121 Tectonophysics: Dynamics, convection currents and mantle plumes; *KEYWORDS:* Venus, Beta, timing, age, modeling, plume

Citation: Vezolainen, A. V., V. S. Solomatov, J. W. Head, A. T. Basilevsky, and L.-N. Moresi, Timing of formation of Beta Regio and its geodynamical implications, *J. Geophys. Res.*, *108*(E1), 5002, doi:10.1029/2002JE001889, 2003.

1. Introduction

[2] Beta Regio is one of several broad rises on the surface of Venus (Figure 1) characterized by relatively recent rift zones and associated volcanism [*Senske et al.*, 1992; *Smrekar et al.*, 1997]. It is a topographic upwelling several thousand kilometers across, rising several kilometers above the surrounding plains, and distinguished from tessera plateaus which are of more ancient age [*Smrekar et al.*, 1997; *Basilevsky and Head*, 1998, 2000a]. Beta Regio is characterized by a major gravity anomaly [*Sjogren et al.*, 1997], and the associated rift zone, Devana Chasma, forms a three-pronged junction near the summit, the site of extensive late-stage volcanic extrusion, Theia Mons [*Senske et al.*, 1992; *Smrekar et al.*, 1997] (Figure 2).

[3] The most likely explanation for the origin of Beta Regio is a hot mantle upwelling [*McGill et al.*, 1981; *Senske et al.*, 1991; *Phillips and Hansen*, 1994; *Stofan et al.*, 1995]. Models of mantle upwelling have been constrained by gravity and topography data [*Kiefer and Hager*, 1991; *Moresi and Parsons*, 1995; *Nimmo and McKenzie*, 1996; *Moore and Schubert*, 1997] and, more recently, by rheological data [*Solomatov and Moresi*, 1996]. In particular, they suggest that the present-day thermal lithosphere in this region is thick, perhaps around 200–400 km. The uncertainties are due to the fact that a range of models (e.g. different Rayleigh numbers) can fit the data equally well. Additional constraints are required to reduce these uncertainties. Other issues, such as where and when the plume formed, remain unclear yet they are critical in distinguishing between various models of global evolution of Venus [*Solomatov and Moresi*, 1996; *Reese et al.*, 1999]. The timing of Beta Regio uplift can provide new constraints on these problems.

2. Timing of Formation of Beta Regio

[4] Detailed geologic mapping [*Basilevsky*, 1996; *Ivanov and Head*, 2001] of the region shows that the background geologic units (tessera, early plains, and regional plains) seem to have formed prior to the development of major topography presently associated with Beta. In these earlier units, the geologic structure and unit distribution is similar to that of many other areas of Venus [*Basilevsky and Head*, 1998, 2000a; *Basilevsky*, 1996; *Ivanov and Head*, 2001]. Subsequent to this, extensive rifting clearly associated with Beta occurred, and associated volcanic deposits show the influence of slopes tilting away from the focus of rifts in central Beta [*Basilevsky*, 1996]. The axial rift of Beta, Devana Chasma, cuts regional plains [*Senske et al.*, 1992; *Basilevsky*, 1996], and clearly indicates that Beta uplift occurred after the emplacement of regional plains. No traces of old, preregional plains rifting are seen within Devana Chasma [*Basilevsky and Head*, 2000b].

[5] Another limit on Beta age can be imposed by the wrinkle-ridge network, which is not concentric to the uplift in Beta Regio [*Basilevsky*, 1996], as it is concentric to the

[1]Department of Physics, New Mexico State University, Las Cruces, New Mexico, USA.
[2]Department of Geological Sciences, Brown University, Providence, Rhode Island, USA.
[3]Vernadsky Institute of Geochemistry and Analytical Chemistry, Russian Academy of Sciences, Moscow, Russia.
[4]Department of Mathematics and Statistics, Monash University, Clayton, Victoria, Australia.

0148-0227/03/2002JE001889$09.00

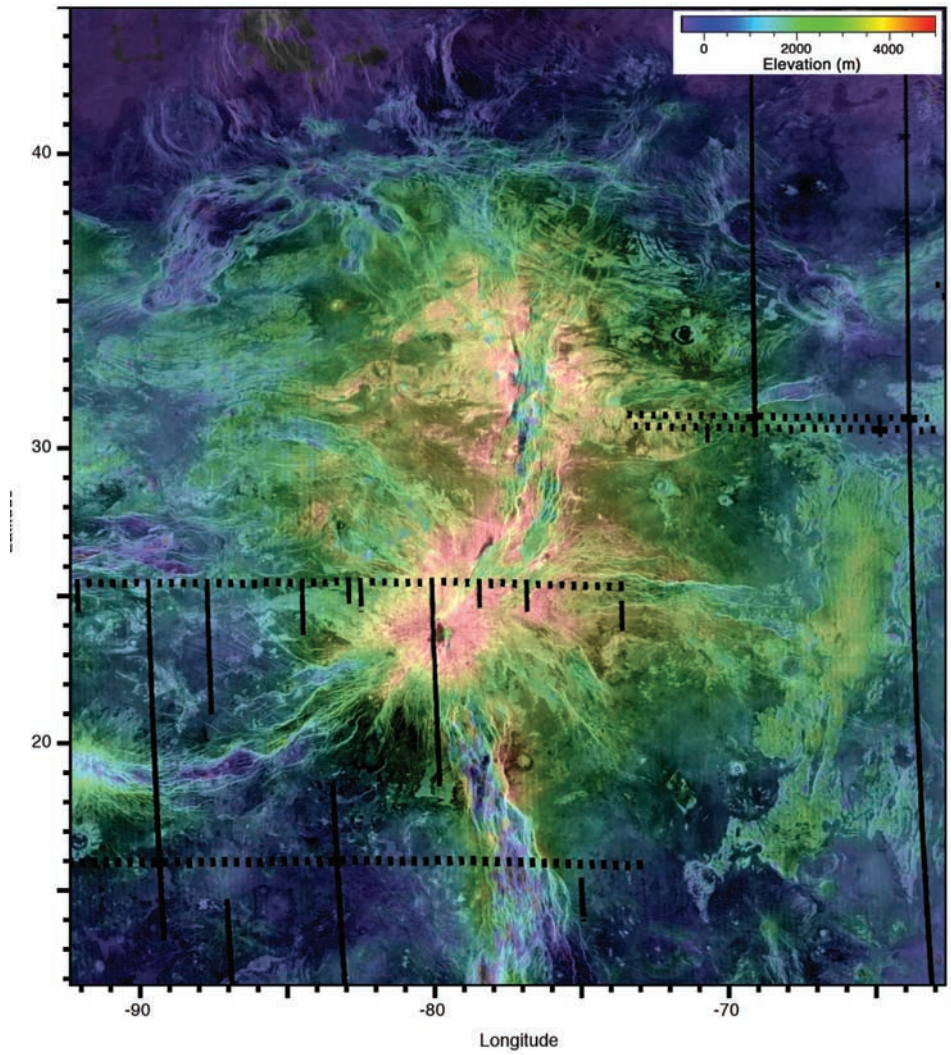

Figure 1. Magellan SAR mosaic of Beta Regio overlain on a color-coded altimetry map and showing the broad topographic rise of Beta Regio, its superposed radial rift zone Devana Chasma, and the summit volcano, Theia Mons. Bright areas in SAR mosaic are relatively rough, and dark areas relatively smooth. Black vertical lines are data gaps, each about 20 km wide. Detailed feature nomenclature for the same area is shown in Figure 2. Simple cylindrical projection centered at ~28N and 284E.

Sif and Gula topographic rise [*Basilevsky*, 1994; *Banerdt et al.*, 1997]. Assuming wrinkle-ridge alignment to be controlled by a combination of regional or global stress and local stress from a topographic load [*Banerdt and Golombek*, 1988], the fact that the ridges are not concentric to Beta implies that the uplift occurred after the emplacement of wrinkle-ridges.

[6] Time of the emplacement of regional plains and their deformation by the wrinkle ridge network is close to the mean surface age of Venus T [*Basilevsky and Head*, 1998; *Basilevsky et al.*, 1999; *Basilevsky and Head*, 2000a]. There is evidence that the emplacement of regional plains and their wrinkle ridging was rather rapid geologically and occurred approximately synchronously all around the planet [see, e.g., *Basilevsky and Head*, 1998, 2000a]. In this case, formation of the Beta uplift should postdate time T ago. However, *Guest and Stofan* [1999] interpreted their observations to favor nonsynchronous (diachronous) emplacement of regional plains. In this case, the mean age of regional plains is still close to T [*Basilevsky and Head*, 1998; *Basilevsky et al.*, 1999; *Basilevsky and Head*, 2000a], although, in a specific area it may differ from T.

[7] Additional constraints on age of Beta come from the analysis of impact craters in this area. The crater Sanger on the northeastern flank of Beta rise (33.77° N, 288.56° E, D = 83.6 km) is superimposed on regional plains and islands of tessera. It has abundant ejecta outflows and a prominent radar-dark halo. To the northeast of the crater its ejecta outflow is cut by a long fault which is part of the Devana Chasma rift zone [*Solomon et al.*, 1992]. Craters with prominent dark halos are estimated to have age less than $0.35T$ [*Herrick and Phillips*, 1994] or less than $\sim 0.5T$ [*Basilevsky and Head*, 2002]. So at least some rifting in Beta area occurred as recently as $0.5T$ ago or later.

[8] Another crater, Olga (26.1° N, 283.8° E, D = 15.5 km) is superposed on regional plains heavily deformed by

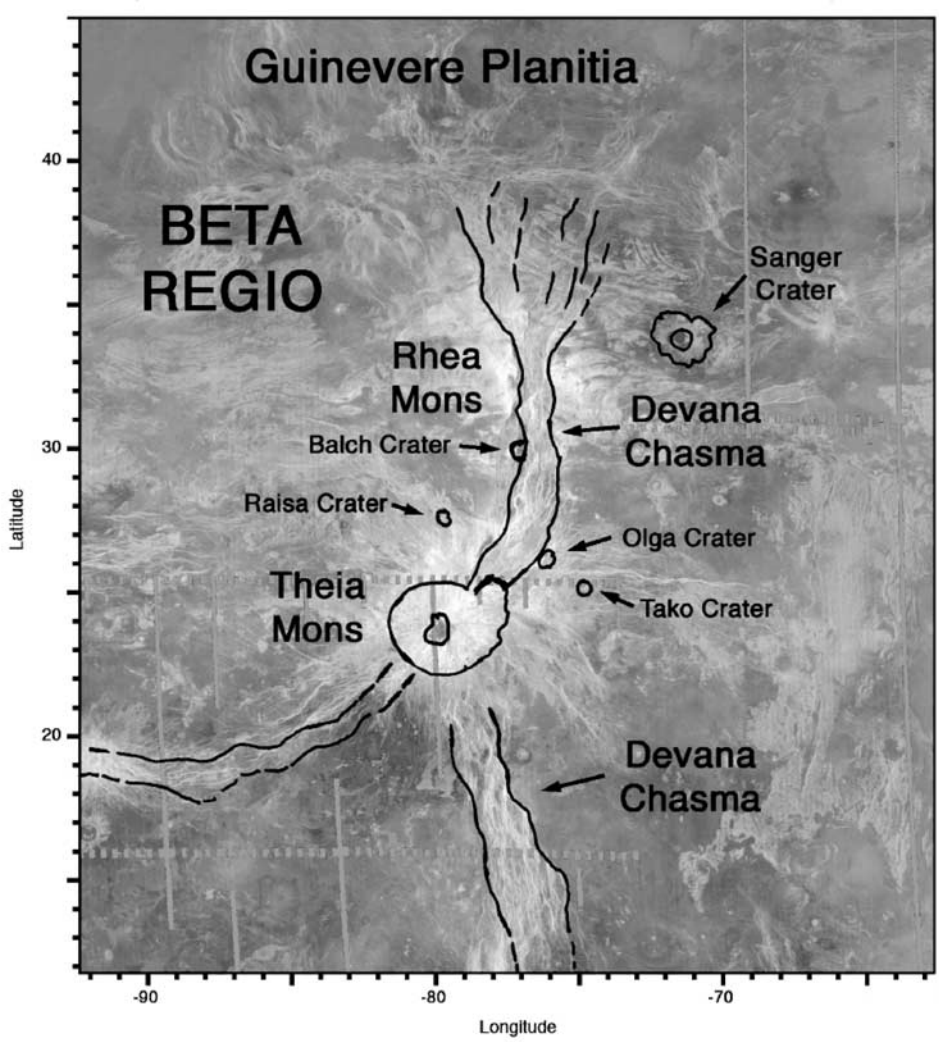

Figure 2. Sketch map of area of Figure 1 showing location and nomenclature of features in Beta Regio.

the Devana rift faults. Blocks of moderately deformed regional plains neighboring the craters are radar dark, and this was interpreted as a crater-associated clear dark halo [*Basilevsky and Head*, 2002]. In this case, the crater should form not earlier than $0.35-0.5T$ ago. The crater Olga is deformed by a younger phase of Devana rifting. This shows that in this case the Devana Chasma rifting was active as recently as $0.5T$ ago or even later.

[9] It is necessary to note that degradation of the crater-associated dark deposit is controlled by the surface processes and thus to a first approximation does not depend on synchronous versus diachronous interpretations of the timing of emplacement of regional plains. So, our estimates that Beta was active at least as recently as $\sim 0.5T$ ago does not depend on the results of the continuing synchronous versus diachronous controversy, e.g. [*Basilevsky et al.*, 1997; *Guest and Stofan*, 1999].

[10] Thus we can conclude that at the time close to T, the Beta uplift and its axial rifting had not yet started, but at the time as recent as $0.35-0.5T$ or even younger, the rifting and obviously uplifting were occurring. The mean age of the Venus surface, T, estimated from impact crater density, is 200–500 m.y. [*Strom et al.*, 1994], 400–800 m.y. [*Phillips et al.*, 1992], 300–750 m.y. [*Schaber et al.*, 1992; *McKinnon et al.*, 1997], or even 400–1600 m.y. [*Zahnle and McKinnon*, 1996]. This gives a wide range 70–800 m.y. for the upper estimate of the age of Beta Regio. Using the average estimates we conclude that at the time 300–750 m.y. ago, Beta uplift and the associated axial rifting, had not yet started, while at the time 100–400 m.y. ago the Beta Regio structure was active.

3. Model

[11] The finite element code CITCOM [*Moresi and Solomatov*, 1995] is used to solve the equations of thermal convection in Boussinesq approximation in 1×1 square box with a fixed temperature contrast ΔT between the lower and upper boundaries. All boundaries are free-slip. The side boundaries are thermally insulated.

[12] The Rayleigh number is defined as

$$Ra_1 = \frac{\alpha g \rho \Delta T d^3}{\kappa \eta_1}, \qquad (1)$$

where ρ is the density, g is the gravity acceleration, α is the thermal expansion, and κ is the thermal diffusivity. η_1 is the viscosity at the lower boundary and d is the thickness of the convective layer.

[13] The viscosity is an Arrhenius function of temperature,

$$\eta = b \exp\left(\frac{Q}{RT}\right), \tag{2}$$

where b is a constant, $Q = E^* + PV^*$ is the activation enthalpy, V^* is the activation volume, P is the hydrostatic pressure, E^* is the activation energy, and R is the universal gas constant.

[14] For large viscosity contrasts and small values of PV^*, equation (2) can be approximated by an exponential function (Frank-Kamenetskii approximation)

$$\eta = \eta_0 \exp(-\gamma T), \tag{3}$$

where η_0 is the viscosity at the upper boundary, $\gamma = E^*/RT^2_i$ is a constant, and T_i is the interior temperature. The difference between the exponential and Arrhenius functions was discussed in detail by *Reese et al.* [1999].

[15] An important controlling parameter is the Frank-Kamenetskii parameter defined as

$$\theta = \gamma \Delta T. \tag{4}$$

[16] The range of θ can be estimated using *Karato and Wu*'s [1993] data for both diffusion (Newtonian viscosity) and dislocation creep (non-Newtonian power law viscosity with the power law exponent $n = 3$ to 3.5). The effect of non-Newtonian viscosity can roughly be approximated with the help of Newtonian viscosity with a reduced activation enthalpy βQ. The estimates of the reduction factor β are: 0.3–0.5 (*Christensen*'s [1984a] direct numerical comparison for $n = 3$), $5/(2n + 3) \approx 0.5$–0.6 (steady state analytical solutions [*Reese et al.*, 1999]) and $3/(n + 2) \approx 0.5$–0.6 (time-dependent solutions [*Solomatov and Moresi*, 2000]). Taking also into account a correction due to pressure-dependent term in the viscosity function [*Reese et al.*, 1999; *Dumoulin et al.*, 1999; *Solomatov and Moresi*, 2000] the range of possible θ is as follows:

$$e^{\theta} = 10^3 - 10^6. \tag{5}$$

[17] We should note that the approximation of Newtonian viscosity in terms of Newtonian viscosity does not capture all the differences between the two rheologies. Among the most substantial differences are that with non-Newtonian viscosity the stagnant lid is nearly flat [*Solomatov and Moresi*, 1997] and that time-dependent convection is characterized by avalanche-like fluctuations [*Larsen et al.*, 1996, 1997; *van Keken*, 1997; *Solomatov and Moresi*, 2000]. The first effect substantially reduces gravity and topography anomalies while the second one generates fast plumes (see additional discussion later).

[18] For the exponential viscosity law (3), θ also determines the viscosity contrast between the upper and lower boundaries: $\Delta\eta = \eta_0/\eta_1$, where η_0 is the surface viscosity.

4. Topography and Geoid Anomalies

[19] Having determined the temperature field in the region, we can find surface geoid and topography anomalies induced by the convective motion. Under free slip boundary conditions at the upper and lower surfaces of the region during the simulations the topography uplift, h_s, is calculated from the vertical normal stress σ_{zz} at the upper boundary as $h_s = -\sigma_{zz}/\rho g$, where ρ is density and g is the gravity, or, in nondimensional variables, as

$$h'_s = -\sigma'_{zz}. \tag{6}$$

[20] Thus, making the change of variable for σ'_{zz} in the equation (6), we get the relation between dimensional and nondimensional topographies $h_s = (\eta_1\kappa/\rho g d^2)\, h'_s$ which can be rewritten as

$$h_s = \frac{\alpha \Delta T d}{Ra_1} h'_s. \tag{7}$$

[21] The nondimensional geoid anomaly is related to the dimensional one as [*Solomatov and Moresi*, 1996]

$$N = \frac{2\pi G \rho \alpha \Delta T d^2}{g Ra_1} N'. \tag{8}$$

[22] The geoid-topography ratio N/h_s obtained from the equations (7) and (8) does not depend on Rayleigh number and is mainly determined by the depth of the layer d, which is the most flexible parameter here:

$$\frac{N}{h_s} = \frac{2\pi G \rho d N'}{g h'_s}. \tag{9}$$

The depth of plume formation can vary from the depth of the core-mantle boundary ($\sim$2800 km) to, perhaps, $\sim$700 km in case of layered mantle convection.

[23] Thus, the depth of the plume formation can be found from equation (9) using the calculated, nondimensional, and the observed geoid to topography ratios [*Solomatov and Moresi*, 1996].

5. Parameters

[24] In order to find dimensional geoid and topography values we take the following parameters for Beta Regio: the density is $\rho = 3300$ kg m^{-3}, gravity acceleration is $g = 8.9$ m s^{-1}, thermal expansion is $\alpha = 3 \cdot 10^{-5}$ K^{-1}, temperature contrast is $\Delta T = 1100$ K, and $\kappa = 8.1 \cdot 10^{-7}$ m^2 s^{-1} is thermal diffusivity [*Solomatov and Moresi*, 1996]. Assuming the observed geoid to topography ratio for Beta Regio to be 30 m km^{-1}, from equation (9) we get for the depth of the layer d, in kilometers:

$$d[\mathrm{km}] = 1.93 \cdot 10^2 \cdot \frac{h'_s}{N'}, \tag{10}$$

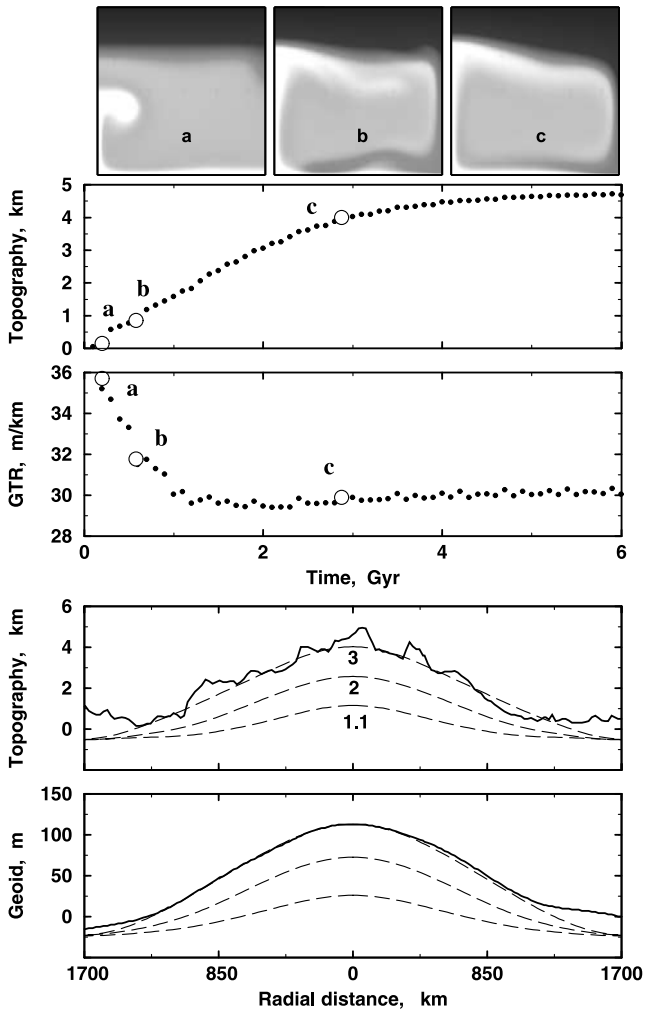

Figure 3. Reference model [*Solomatov and Moresi*, 1996]. Rayleigh number $Ra_1 = 3 \cdot 10^7$, viscosity contrast is 10^6. Topography uplift and geoid-topography ratio as functions of time. Temperature fields are shown at the times a, b, and c. Calculated depth of plume formation $d \sim 1670$ km. Convection gradually approaches the steady-state solution described by *Solomatov and Moresi* [1996]. Topography and geoid (dashed lines) at 1.1, 2, and 3 b.y. are superimposed on Magellan profiles across Beta Regio (solid lines).

where h_s'/N' is the calculated nondimensional topography to geoid ratio.

6. A Reference Model

[25] We start with a reference model: viscosity contrast of 10^6 and bottom Rayleigh number of $Ra_1 = 3 \cdot 10^7$. This is a model from the range of steady state models which give good agreement with the gravity and topography of Beta Regio and also satisfy experimental constraints on the viscosity law [*Solomatov and Moresi*, 1996].

[26] For a time-dependent model, both the average interior temperature and the bottom temperature are taken from the reference model. The only difference is that the lid is initially flat, with temperature linearly varied from zero at the upper surface of the region to the average interior temperature at the bottom of the lid.

[27] We add a small (1%) harmonic perturbation to the temperature field to initiate plume formation. Perturbations grow at the bottom of the region. Then the plume moves upward relatively fast, reaches the lid, heats the lid and eventually approaches the equilibrium thermal state which corresponds exactly to the reference model (Figure 3).

[28] We calculate topography in the accordance with the equations (6) and (7) and geoid to topography ratio is defined as an admittance at the largest wavelength $\lambda/2 = d$, where d is the height of the 1×1 region.

[29] It is interesting to note that the geoid to topography ratio approaches its steady state value much faster than it takes for the topography itself to rise to its steady state value. As soon as the plume formed by the initial perturbation has reached the lid, the topography-geoid ratio tends to be close to its steady state level (Figure 3).

[30] We find that it takes about 3 billion years for the topography to approach the present-day topography of Beta Regio (Figure 3) (note that the depth of the layer is about 1700 km which is required to fit simultaneously both topography and gravity for Beta Regio [*Solomatov and Moresi*, 1996]). This large time-scale is inconsistent with the geological constraints. Below we consider several factors which could affect the uplift rate.

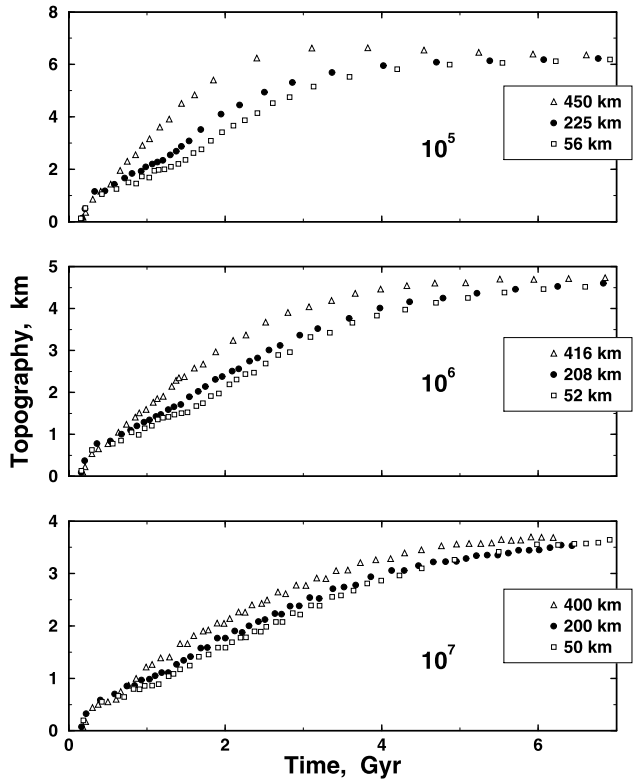

Figure 4. Dimensional topography uplifts as functions of time at $Ra_1 = 3 \cdot 10^7$ and different viscosity contrasts and initial lid thicknesses. To fit both gravity and topography to their present-day values the depths of the plume formation are chosen to be 1800, 1670, and 1600 km for viscosity contrasts 10^5, 10^6, and 10^7 respectively.

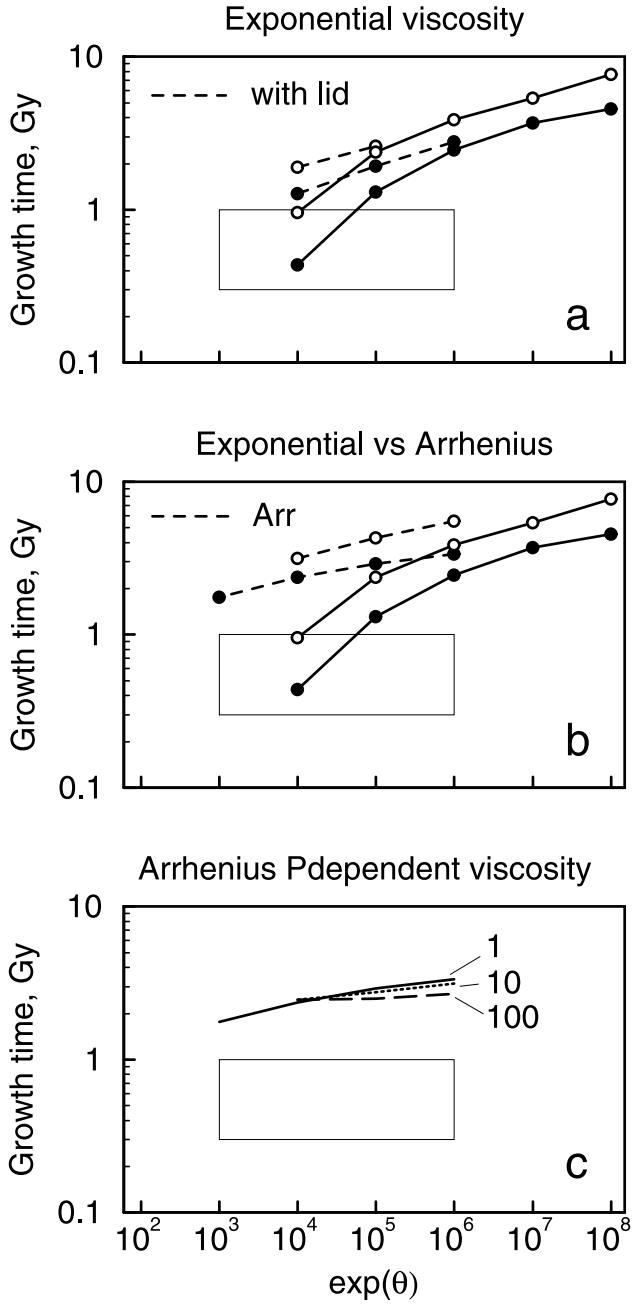

Figure 5. The dependence of the growth time for Beta Regio as a function of exp(θ) for various viscosity laws. (a) Exponential viscosity law. The Rayleigh number is $Ra_1 = 1 \cdot 10^7$ (open circles) and $3 \cdot 10^7$ (solid circles). The dashed lines show how the results change in the presence of a very viscous lid at the surface of the layer. (b) Arrhenius law (dashed lines) versus exponential law (solid lines). The Rayleigh number is $Ra_1 = 1 \cdot 10^7$ (open circles) and $3 \cdot 10^7$ (open circles). (c) Arrhenius pressure-dependent viscosity. The labels indicate the pressure-induced viscosity contrast between the bottom of the layer and the bottom of the lid. The Rayleigh number defined at the viscosity at the bottom of the stagnant lid is $3 \cdot 10^7$ in all three cases. The total viscosity contrast across the layer (due to temperature) is 10^8 in all cases with Arrhenius viscosity. The box shows the parameter range which satisfies both the rheological constraints and the timing of formation of Beta Regio.

7. Simulation of the Uplift

7.1. Initial Conditions

[31] The amplitude of the initial perturbation does not seem to affect much the growth rate of the upwelling. The gravity anomaly as well as the topography associated with this initial stage do not exceed 20% of their steady state values (Figure 3). The duration of the initial plume formation and its movement through the depth of the region, in all cases, is less than 5–10% of the time for the convection to reach steady state (Figure 3). Although a strong plume (e.g. initiated by a large perturbation at the lower boundary of the region) penetrates the mantle faster, the uplift growth time will be just 10% less.

[32] The initial thickness of the lid also has affect the growth rate. Counter-intuitively, thinner initial lids give somewhat larger growth times (Figure 4). This happens because gravity and topography anomalies are caused by variations in the lid thickness. To produce the observed magnitude of the anomaly, the lid needs to grow back to its steady state thickness. Therefore, an initially thin lid slows down the uplift. For example, reducing the initial lid thickness by half, the uplift time increases from 3 to 4 billion years.

[33] In our further simulations we keep the initial lid thickness close to the equilibrium (about $0.25d$).

7.2. Rayleigh Number

[34] The uplift rate strongly depends on the Rayleigh number and the viscosity law (Figure 5). In general, larger Rayleigh numbers imply a larger force at the base of the lithosphere and smaller viscosity contrasts imply a smaller resistance in the lithosphere. Both factors accelerate the flow in the lower part of the lithosphere, and, thus, the uplift rate.

[35] The results for the model with the highest uplift rate are presented in Figure 6. This model has an exponential viscosity law with the viscosity contrast 10^4. The Rayleigh number is $Ra_1 = 3 \cdot 10^7$. The uplift time is ~500 m.y. which is consistent with geological constraints. The present-day lithospheric thickness, defined by the maximum gradient of the vertical velocity (Figure 7), is about 340 km just above the plume head. According to this model, Beta Regio is still growing (Figure 8).

[36] Although the model is in agreement with geological constraints it rises several questions. First of all, when the viscosity contrast is as low as 10^4, Frank-Kamenetskii approximation is inaccurate in predicting growth rates. A related problem is that the motion of the lid as a whole starts affecting the convective flow [*Solomatov*, 1995]. The shape of the final steady state profiles of the topography and the geoid points to the same problem [see, e.g., *Solomatov and Moresi*, 1996, Figure 6]. It seems that the flow changes from stagnant lid regime to a mobile lid regime (transitional regime) during the uplift. In addition, a soft and mobile Venusian lithosphere is difficult to reconcile with the high strength of the crust [*Mackwell et al.*, 1998].

7.3. Exponential Versus Arrhenius Viscosity

[37] To eliminate the problems related with Frank-Kamenetskii approximation and to keep the flow in the stagnant lid convection regime, we considered the original Arrhenius viscosity law (2). However, unless we assume extremely low values of the Frank-Kamenetskii parameter the uplift

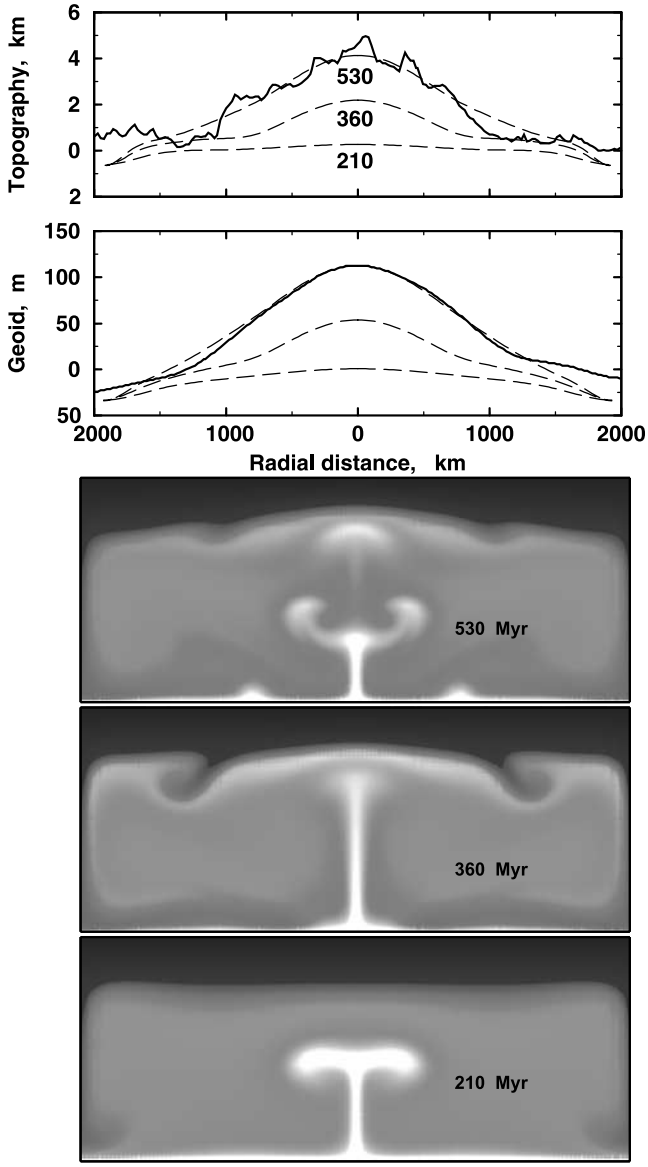

Figure 6. Calculated topography and geoid at $t = 210$, 360 and 530 million years (dashed lines) compared to the topography and geoid profiles across Beta Regio (solid lines). The Rayleigh number is $Ra_1 = 3 \cdot 10^7$ and the viscosity contrast is 10^4. Calculated depth of plume formation $d \sim 1920$ km, Lid thickness at 530 m.y. is $\sim$340 km.

rates are much slower than those obtained with the exponential viscosity (Figure 5b). These results suggest that to obtain fast uplift rates, the lithosphere must be very weak.

7.4. Rheologically Stratified Lithosphere

[38] It is also possible that only the lower part of the lithosphere is weak while the upper layers remain strong. To simulate this situation we consider an exponential viscosity law and impose a thin, very viscous layer near the surface (Figure 9). This immobilizes the surface and yet allows flow in the lower part of the lithosphere. This also enforces the stagnant lid convection regime playing the same role as rigid boundary conditions [*Davaille and Jaupart*, 1994]. Although the uplift rates are substantially reduced (Figure 5a), they can still be reconciled with geological constraints.

7.5. Pressure-Dependent Viscosity

[39] Pressure-dependent viscosity can also affect the uplift rates. To evaluate the role of this factor, we consider an Arrhenius viscosity law with the parameters chosen in such a way as to obtain the same viscosity and the same effective Frank-Kamenetskii parameter at the bottom of the lid [*Reese et al.*, 1999; *Dumoulin et al.*, 1999; *Solomatov and Moresi*, 2000]. Since this choice of parameters ensures that the viscosity law near the bottom of the lid remains the same and since the viscosity in the upper parts of the lid does not affect the results, the effect of pressure-dependent viscosity in the deep mantle is now well isolated. We find that pressure-dependent viscosity does not affect much the uplift rates for the pressure-induced viscosity contrasts of up to 100 (Figure 5c).

8. Other Factors which Can Affect the Uplift Rate

8.1. Dislocation Creep

[40] Non-Newtonian viscosity (dislocation creep) strongly affects convection. Avalanche-like instabilities produce strong upwellings and downwellings which can propagate very fast across the convective layer [*Larsen et al.*, 1996, 1997; *van Keken*, 1997; *Solomatov and Moresi*, 2000]. However, the stresses are never large enough to move the viscous lid (provided we remain in the parameter space constrained by laboratory data) - this is what is really necessary for a fast uplift. Moreover, for non-Newtonian viscosity the thermal thinning of the lithosphere is very small [*Solomatov and Moresi*, 1997]. As a result, the steady state gravity and topography anomalies are much smaller than for Newtonian viscosity. For example, in the set of non-Newtonian models described by *Solomatov and Moresi* [1997] and *Reese et al.* [1999] the topography and gravity in the stagnant lid regime are about 3 to 10 times smaller than the observed values for Beta (for the admittance of 30 m/km). Within the limits of our square-box model, non-Newtonian viscosity cannot give the required topography and gravity of Beta Regio.

8.2. Transient Creep

[41] The transient creep (before the steady state dislocation creep is reached) reduces the apparent viscosity and can increase the uplift rates. However, the effect is unlikely to be substantial: the viscosity in the transient creep is only a factor of 2 to 10 smaller than that in the steady state creep [*Carter and Kirby*, 1978; *Hansen and Spetzler*, 1994; *Chopra*, 1997].

8.3. Melting

[42] Melting is another possible mechanism of lithospheric weakening. Melting could have happened due to widespread magmatism during the global resurfacing of Venus [*Reese et al.*, 1999]. However, the situation is not obvious: the reduction in the viscosity is less than one order of magnitude at the melt fractions of several percent [*Hirth and Kohlstedt*, 1995a, 1995b; *Kohlstedt and Zimmerman*, 1996] while at higher melt fractions the melt escapes fast on the observed timescale of the uplift [*Solomatov and Stevenson*, 1993; *Solomatov*, 2000]. Therefore, it is unclear

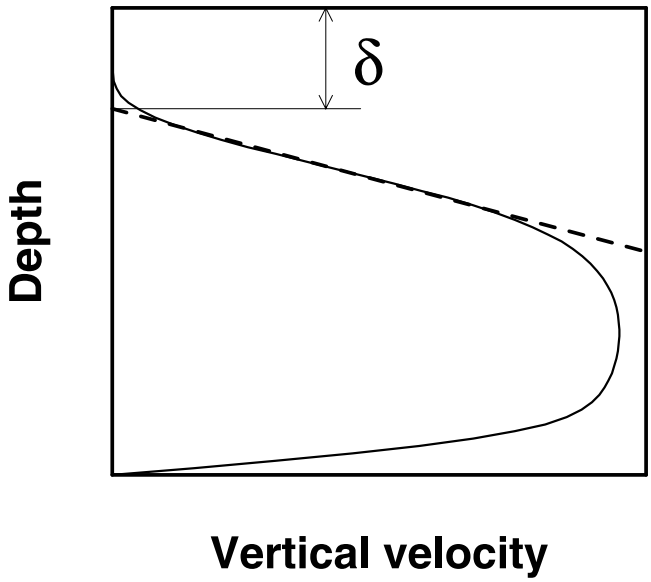

Figure 7. The lithospheric thickness δ is determined from the vertical velocity gradient.

whether melting can substantially accelerate the uplift. Moreover, the reduction in the viscosity due to the presence of melt can be compensated by the increase in the viscosity due to melting-induced dehydration [*Karato*, 1986; *Hirth and Kohlstedt*, 1996; *Karato and Jung*, 1998] Two-phase plumes with realistic rheology are still beyond the capabilities of the existing models.

8.4. Surface Temperature

[43] The increase in the surface temperature due to widespread magmatism and the associated degassing [*Solomon et al.*, 1999; *Phillips et al.*, 2001; *Bullock and Grinspoon*, 2001] could also have played some role in reducing the viscosity of the lithosphere. However, 100 to 200 K temperature increase would change the Frank-Kamenetskii parameter by only 10 to 20% while the lithospheric viscosity would still be too high to mobilize the lithosphere. This implies that this case is within the parameter range studied.

8.5. Three-Dimensional Plumes

[44] To increase the growth rate further, it seems necessary to increase the Rayleigh number or to reduce further Frank-Kamenetskii parameter. However, in those cases convection pattern becomes time-dependent and interpretation of growth rates becomes problematic. As the bottom Rayleigh number Ra_1 approaches 10^8 the flow pattern reshapes. As a new cold plume is sinking near the center of the region, surface topography is losing its bell-like shape and a depression in the topography appears (Figure 10). The spacing between plumes is also likely to change with the Rayleigh number and the viscosity contrasts and, thus, the results depend on the geometry of the numerical domain. This means that fully three-dimensional models need to be investigated.

[45] Axisymmetric models give some insight into what can be expected in three dimensions. Although large viscosity contrasts have not been investigated, models with constant viscosity and small viscosity contrasts [*Kiefer and Hager*, 1992; *King*, 1997] show that peak-to-peak topography and geoid in steady state simulations increase by no more than a factor of 2 (including both spherical and cylindrical axisymmetric models). Our preliminary tests showed that the uplift rates increase by roughly the same amount.

8.6. Small-Scale Convection

[46] Perhaps, the most promising factor which can significantly accelerate the uplift rate of Beta Regio is small-scale convection within the upwelling. In this case, thermal thinning is caused not by thermal diffusion and not by lateral flow in the lithosphere but by small-scale convective insta-

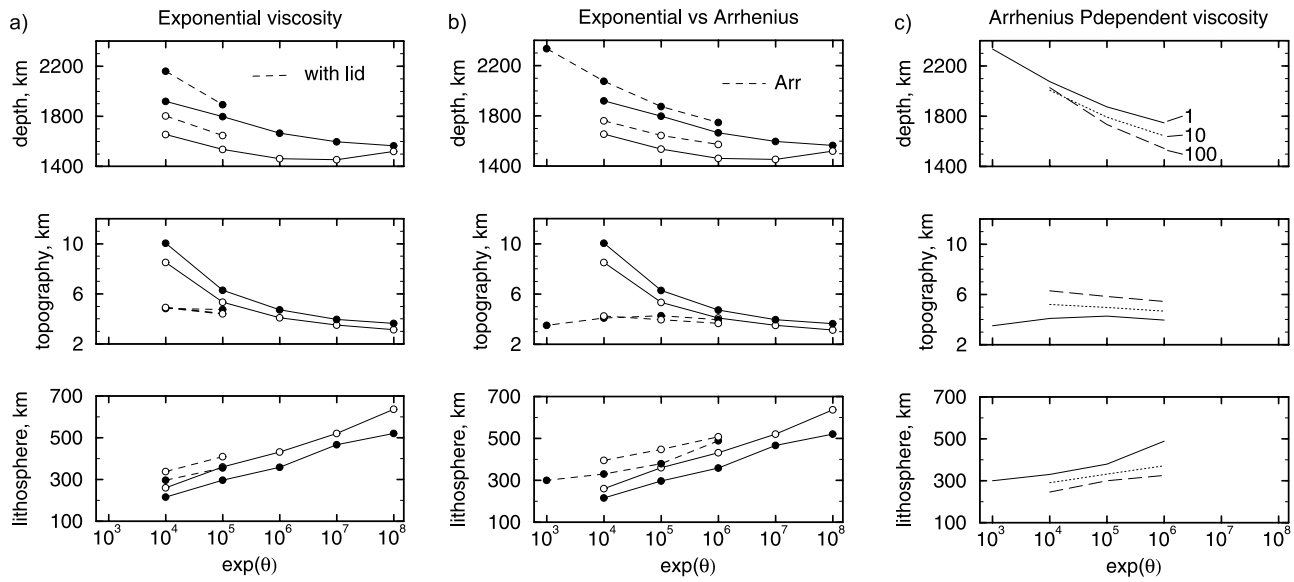

Figure 8. The depth of plume formation, the surface topography, and the lithospheric thickness for Beta Regio are shown for the models from Figure 5 and for $t = \infty$ (steady-state results): (a) Exponential viscosity (with and without viscous lid), (b) Arrhenius versus exponential law and (c) Arrhenius pressure-dependent viscosity.

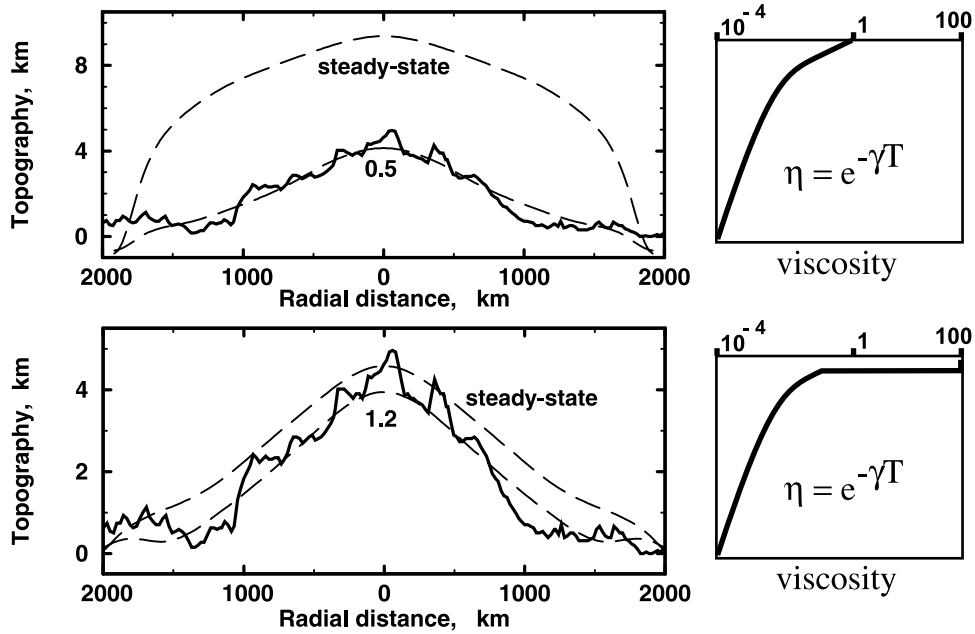

Figure 9. The effect of a strong viscous lid on top of the layer on the topography and growth rate of Beta Regio. Rayleigh number Ra_1 is $3 \cdot 10^7$. Uplift times are shown in 10^9 years.

bilities at the bottom of the lithosphere. This process can erode the lithosphere very fast. This can happen in two ways: (i) Small-scale instabilities can occur within the plume head like in three-dimensional simulations by *Moore et al.* [1998, 1999]; (ii) Small-scale instabilities can develop at the bottom of the lithosphere without any plume, during the conductive cooling of the planet. Because of pressure-dependent viscosity, the equilibrium lithospheric thickness is located at a shallower depth. The instabilities quickly propagate upward until the lithospheric thickness reaches its stable equilibrium.

8.7. Large Temperature Contrasts Across the Bottom Boundary Layer

[47] We considered only moderate temperature contrast across the bottom boundary layer. A different type of upwelling can be generated when the temperature contrast exceeds the critical one for initiation of small-scale convection within the boundary layer itself [*Yuen and Peltier*, 1980; *Christensen*, 1984b; *Olson et al.*, 1987; *Thompson and Tackley*, 1998; *Solomatov and Moresi*, 2002]. The plumes generated in this case can be very large. This can increase the uplift rates. It is unclear whether such temperature differences (~1000 K) are realistic for Venus but a large viscosity of the lower mantle compared to the upper mantle is one possible way to produce large temperature differences in the bottom boundary layer. This is certainly the case for the Earth [e.g., *King*, 1995]. This problem would be interesting to investigate in the future.

8.8. Viscous Relaxation of the Lid

[48] At large viscosity contrasts most of the convective parameters including gravity and topography do not depend

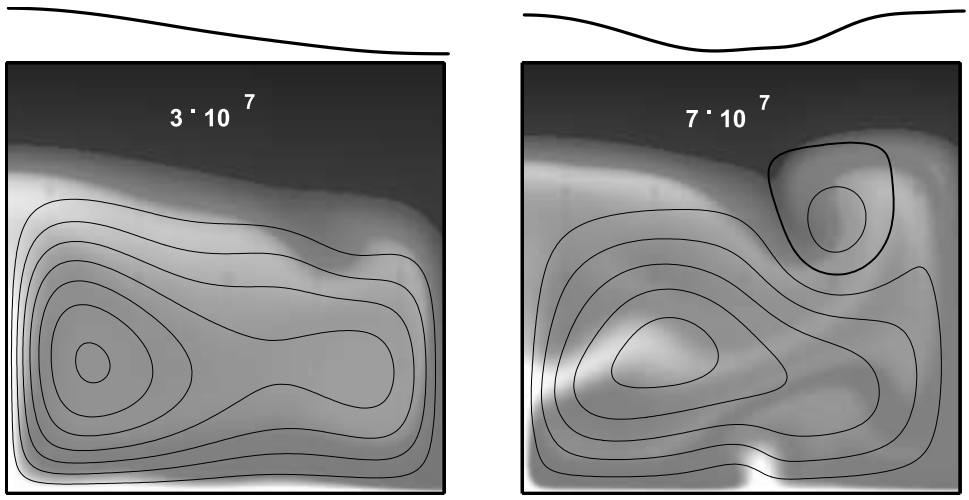

Figure 10. Transition to time-dependent convection. Temperature field and the stream line function are shown for the viscosity contrast $\Delta\eta = 10^7$ and the Rayleigh numbers $Ra_1 = 3 \cdot 10^7$ and $7 \cdot 10^7$. The curves above the convective regions is the topography.

on the viscosity of the upper parts of the lithosphere. However, the topography is calculated from the vertical stresses on the upper free-slip boundary which involves the assumption of an instant reaction of lithosphere to a load. This assumption is valid only if the evolution of temperature field in the region is relatively slow compared to the time required for the topography to respond to a fixed load. A thick and very viscous lithosphere can significantly reduce the uplift rates [*Zhong et al.*, 1996]. Below we investigate the role of this effect and estimate the viscosity range in which our model is valid.

[49] Let the lithosphere be a plate of viscosity η_L and thickness δ floating on a mantle of viscosity η_M. Vertical deflection w of a thin viscous plate subjected to a load provided by topography h and pressure at the lithosphere-mantle boundary can be described as [e.g. *Turcotte and Schubert*, 2002]

$$-\frac{\eta_L \delta^3}{3}\frac{\partial^5 w}{\partial x^4 \partial t} = \rho g h + \frac{4\pi\eta_M}{\lambda}\frac{\partial w}{\partial t}, \tag{11}$$

where λ is the characteristic topography wavelength. For the case when the deflection rate is controlled by the viscosity of the lithosphere, we get the following scaling law:

$$t = 10^{-3}\frac{\eta_L \delta^3}{\rho g \lambda^4}, \tag{12}$$

where the coefficient is chosen to fit the numerical results from [*Zhong et al.*, 1996].

[50] Our model is valid if the uplift time given by equation (12) is less than the characteristic convection timescale ~100 m.y.,

$$\eta_L < 10^{26}\ \text{Pa s}, \tag{13}$$

where η_L is some average viscosity of the lithospheric plate. If the viscosity of the lid is larger than (13), then the uplift is slower than our models predict.

8.9. Elastic Effects

[51] Elasticity should be taken into account for rapid processes, when the characteristic time of a process is smaller than Maxwell relaxation time η/E, where E is the Young's modulus. If elastic properties of the lithosphere of Venus are similar to that of the Earth, then $E \sim 10^{11}$ Pa and elasticity can be ignored if $\eta < 10^{26}$ Pa s which coincides with the condition (13).

9. Conclusion

[52] We simulated the formation of Beta Regio due to a thermal plume and explored several factors. The best results are obtained for the model with exponential viscosity law and the viscosity contrast of 10^4. This model predicts correct gravity and topography anomalies and fast uplift time for Beta Regio, ~500 million years, consistent with geological constraints. It also suggests that the uplift continues at present times. However, it is difficult to reconcile such small viscosity contrasts with experimental data on the rheology of rocks. Furthermore, the lateral flow of the lithosphere in this model implies that the lithosphere becomes partially mobilized - the regime which may not be applicable to Venus. A similar model but with a strong upper crust immobilizes the lithosphere. It gives the uplift time of about 1.2 b.y. and is marginally acceptable from both geological and geodynamical points of view. In any case, to satisfy the geological constraints on the uplift rate of Beta, the lithosphere or at least its lower part must be "softer" than expected at subsolidus temperatures. There are two possible interpretations of these results: (i) The model needs to be substantially modified. The most promising effect is small-scale convection which can develop in the plume [*Moore et al.*, 1998, 1999] or in some other type of upwelling [*Reese et al.*, 1999]; (ii) The lithosphere is, indeed, weak. Its strength may not be much higher than on Earth for which the estimates of the viscosity contrasts between the mantle and the lithosphere usually fall below 10^4 [*Kaula*, 1980; *Bills et al.*, 1994; *Molnar and Gipson*, 1996; *England and Molnar*, 1997; *Flesch et al.*, 2000].

[53] **Acknowledgments.** We thank the reviewers for their insightful comments. This work was supported by NASA.

References

Banerdt, W. B., and M. P. Golombek, Deformational models of rifting and folding on Venus, *J. Geophys. Res.*, *93*, 4759–4772, 1988.

Banerdt, W. B., G. E. McGill, and M. T. Zuber, Plains tectonics on Venus, in *Venus II*, edited by S. W. Bougher, D. M. Hunten, and R. J. Phillips, pp. 901–930, Univ. of Ariz. Press, Tucson, 1997.

Basilevsky, A. T., Concentric wrinkle ridge pattern around Sif and Gula (abstract), *Proc. Lunar Planet. Sci. Conf. 25th*, 63–64, 1994.

Basilevsky, A. T., Geologic mapping of V17 Beta Regio quadrangle: Preliminary results, *Lunar Planet. Sci.*, *XXVII*, 65–66, 1996.

Basilevsky, A. T., and J. W. Head, The geologic history of Venus: A stratigraphic view, *J. Geophys. Res.*, *103*(E4), 8531–8544, 1998.

Basilevsky, A. T., and J. W. Head, Geologic units on Venus: Evidence for their global correlation, *Planet. Space Sci.*, *48*, 75–111, 2000a.

Basilevsky, A. T., and J. W. Head, Rifts and volcanoes of Venus: Global assessment of their age relations with regional plains, *J. Geophys. Res.*, *105*(E10), 30,123–30,139, 2000b.

Basilevsky, A. T., and J. W. Head, Venus: Analysis of the degree of impact crater deposit degradation and assessment of its use for dating geological units and features, *J. Geophys. Res.*, *107*(E8), 5061, doi:10.1029/2001JE001584, 2002.

Basilevsky, A.T., A. T., J. W. Head, G. G. Schaber, and R. G. Strom, The resurfacing history of Venus, in *Venus II*, edited by S. W. Bougher, D. M. Hunten, and R. J. Phillips, pp. 1047–1084, Univ. of Ariz. Press, Tucson, 1997.

Basilevsky, A. T., J. W. Head, M. A. Ivanov, and V. P. Kryuchkov, Impact craters on geologic units of northern Venus: Implications for the duration of the transition from tessera to regional plains, *Geophys. Res. Lett.*, *26*, 2593–2596, 1999.

Bills, B. C., D. R. Curry, and G. A. Marshall, Viscosity estimates for the crust and upper mantle from patterns of lacustrine shoreline deformation in the Eastern Great Basin, *J. Geophys. Res.*, *99*, 20,259–20,286, 1994.

Bullock, M. A., and D. H. Grinspoon, The recent evolution of climate on Venus, *Icarus*, *150*, 19–37, 2001.

Carter, N. L., and S. H. Kirby, Transient creep and semibrittle behavior of crystalline rocks, *Pure Appl. Geophys.*, *116*, 807–839, 1978.

Chopra, P. N., High-temperature transient creep in olivine rocks, *Tectonophys.*, *279*, 93–111, 1997.

Christensen, U. R., Convection with pressure- and temperature-dependent non-Newtonian rheology, *Geophys. J. R. Astron. Soc.*, *77*, 343–384, 1984a.

Christensen, U., Instability of a hot boundary layer and initiation of thermochemical plumes, *Ann. Geophys.*, *2*, 311–320, 1984b.

Davaille, A., and C. Jaupart, Onset of thermal convection in fluids with temperature-dependent viscosity: Application to the oceanic mantle, *J. Geophys. Res.*, *99*, 19,853–19,866, 1994.

Dumoulin, C., M. P. Doin, and L. Fleitout, Heat transport in stagnant lid convection with temperature- and pressure-dependent Newtonian or non-Newtonian rheology, *J. Geophys. Res.*, *104*, 12,759–12,777, 1999.

England, P., and P. Molnar, Active deformation of Asia: From kinematics to dynamics, *Science*, *278*, 647–650, 1997.

Flesch, L. M., W. E. Holt, A. J. Haines, and B. Shen-Tu, Dynamics of the Pacific-North American boundary in the Western United States, *Science*, *287*, 814–834, 2000.

Guest, J. E., and E. R. Stofan, A new view of the stratigraphic history of Venus, *Icarus*, *139*, 55–66, 1999.
Hansen, D. R., and H. A. Spetzler, Transient creep in natural and synthetic, iron-bearing olivine single crystals: Mechanical results and dislocation microstructures, *Tectonophysics*, *235*, 293–315, 1994.
Herrick, R. R., and R. J. Phillips, Implications of a global survey of Venusian impact craters, *Icarus*, *111*, 387–416, 1994.
Hirth, G., and D. L. Kohlstedt, Experimental constraints on the dynamics of the partially molten upper mantle: Deformation in the diffusion creep regime, *J. Geophys. Res.*, *100*, 1981–2001, 1995a.
Hirth, G., and D. L. Kohlstedt, Experimental constraints on the dynamics of the partially molten upper mantle, 2, Deformation in the dislocation creep regime, *J. Geophys. Res.*, *100*, 15,441–15,449, 1995b.
Hirth, G., and D. L. Kohlstedt, Water in the oceanic upper mantle: Implications for rheology, melt extraction and the evolution of the lithosphere, *Earth Planet. Sci. Lett.*, *144*, 93–108, 1996.
Ivanov, M. A., and J. W. Head, Geology of Venus: Mapping of a global geotraverse at 30°N latitude, *J. Geophys. Res.*, *106*, 17,515–17,566, 2001.
Karato, S.-I., Does partial melting reduce the creep strength of the upper mantle?, *Nature*, *319*, 309–310, 1986.
Karato, S.-I., and H. Jung, Water, partial melting and the origin of the seismic low velocity and high attenuation zone in the upper mantle, *Earth Planet. Sci. Lett.*, *157*, 193–207, 1998.
Karato, S.-I., and P. Wu, Rheology of the upper mantle: A synthesis, *Science*, *260*, 771–778, 1993.
Kaula, W. M., Material properties for mantle convection consistent with observed surface fields, *J. Geophys. Res.*, *85*, 7031–7044, 1980.
Kiefer, W. S., and B. H. Hager, A mantle plume model for the equatorial highlands of Venus, *J. Geophys. Res.*, *96*, 20,947–20,966, 1991.
Kiefer, W., and B. Hager, Geoid anomalies and dynamic topography from convection in cylindrical geometry: Application to mantle plumes on Earth and Venus, *Geophys. J. Int.*, *108*, 198–214, 1992.
King, S. D., Models of mantle viscosity, in *Mineral Physics and Crystallography: A Handbook of Physical Constants*, edited by T. J. Ahrens, pp. 227–236, AGU, Washington, D. C., 1995.
King, S. D., Geoid and topographic swells over temperature-dependent thermal plumes in spherical-axisymmetric geometry, *Geophys. Res. Lett.*, *24*, 3093–3096, 1997.
Kohlstedt, D. L., and M. E. Zimmerman, Rheology of partially molten mantle rocks, *Annu. Rev. Earth Planet. Sci.*, *24*, 41–62, 1996.
Larsen, T. B., D. A. Yuen, A. V. Malevsky, and J. L. Smedsmo, Dynamics of strongly time-dependent convection with non-Newtonian temperature-dependent viscosity, *Phys. Earth Planet. Inter.*, *94*, 75–103, 1996.
Larsen, T. B., D. A. Yuen, J. L. Smedsmo, and A. V. Malevsky, Generation of fast timescale phenomena in thermo-mechanical processes, *Phys. Earth Planet. Inter.*, *102*, 213–222, 1997.
Mackwell, S. J., M. E. Zimmerman, and D. L. Kohlstedt, High-temperature deformation of dry diabase with application to tectonics on Venus, *J. Geophys. Res.*, *103*, 975–984, 1998.
McGill, G. E., S. J. Steenstrup, C. Barton, and P. G. Ford, Continental rifting and the origin of Beta Regio Venus, *Geophys. Res. Lett.*, *8*, 737–740, 1981.
McKinnon, W. B., K. J. Zahnle, B. A. Ivanov, and H. J. Melosh, Cratering on Venus: Models and Observations, in *Venus II*, edited by S. W. Bougher, D. M. Hunten, and R. J. Phillips, pp. 969–1014, Univ. of Ariz. Press, Tucson, 1997.
Molnar, P., and J. M. Gipson, A bound on the rheology of continental lithosphere using very long baseline interferometry: The velocity of south China with respect to Eurasia, *J. Geophys. Res.*, *101*, 545–553, 1996.
Moore, W. B., and G. Schubert, Venusian crustal and lithospheric properties from nonlinear regressions of highland geoid and topography, *Icarus*, *128*(2), 415–428, 1997.
Moore, W. B., G. Schubert, and P. Tackley, Three-dimensional simulations of plume-lithosphere interaction at the Hawaiian swell, *Science*, *279*, 1008–1011, 1998.
Moore, W. B., G. Schubert, and P. J. Tackley, The role of rheology in lithospheric thinning by mantle plumes, *Geophys. Res. Lett.*, *26*, 1073–1076, 1999.
Moresi, L., and B. Parsons, Interpreting gravity, geoid and topography for convection with temperature dependent viscosity: Application to surface features on Venus, *J. Geophys. Res.*, *100*(E10), 21,155–21,172, 1995.
Moresi, L.-N., and V. S. Solomatov, Numerical investigation of 2D convection with extremely large viscosity variations, *Phys. Fluids*, *7*, 2154–2162, 1995.
Nimmo, F., and D. McKenzie, Modeling plume-related uplift, gravity and melting on Venus, *Earth Planet. Sci. Lett.*, *145*, 109–123, 1996.
Olson, P., G. Schubert, and C. Anderson, Plume formation in the D"-layer and the roughness of the core-mantle boundary, *Nature*, *327*, 409–413, 1987.
Phillips, R. J., and V. L. Hansen, Tectonic and magmatic evolution of Venus, *Annu. Rev. Earth Planet. Sci.*, *22*, 597–654, 1994.
Phillips, R. J., R. F. Raubertas, R. E. Arvidson, I. C. Sarkar, R. R. Herrick, N. Izenberg, and R. E. Grimm, Impact craters and Venus resurfacing history, *J. Geophys. Res.*, *97*(E10), 15,923–15,948, 1992.
Phillips, R. J., M. A. Bullock, and S. A. Hauck II, Climate and interior coupled evolution on Venus, *Geophys. Res. Lett.*, *28*, 1779–1782, 2001.
Reese, C. C., V. S. Solomatov, and L.-N. Moresi, Non-Newtonian stagnant lid convection and magmatic resurfacing on Venus, *Icarus*, *139*, 67–80, 1999.
Schaber, G. G., R. G. Strom, H. J. Moore, L. A. Soderblom, R. L. Kirk, D. J. Chadwick, D. D. Dawson, L. R. Gaddis, J. M. Boyce, and J. Russell, Geology and distribution of impact craters on Venus—What are they telling us?, *J. Geophys. Res.*, *97*(E8), 13,257–13,301, 1992.
Senske, D. A., J. W. Head, E. R. Stofan, and D. B. Campbell, Geology and structure of Beta Regio, Venus—Results from Arecibo radar imaging, *Geophys. Res. Lett.*, *18*, 1159–1162, 1991.
Senske, D. A., G. G. Schaber, and E. R. Stofan, Regional topographic rises on Venus: Geology of western Eistla Regio and comparison to Beta Regio and Atla Regio, *J. Geophys. Res.*, *97*(E8), 13,395–13,420, 1992.
Sjogren, W. L., W. B. Banerdt, P. W. Chodas, A. S. Konopliv, G. Balmino, J. P. Barriot, J. Arkani-Hamed, T. R. Colvin, and M. E. Davies, The Venus gravity field and other geodetic parameters, in *Venus II*, edited by S. W. Bougher, D. M. Hunten, and R. J. Phillips, pp. 1125–1162, Univ. of Ariz. Press, Tucson, 1997.
Smrekar, S. E., W. S. Kiefer, and E. R. Stofan, Large volcanic rises on Venus, in *Venus II*, edited by S. W. Bougher, D. M. Hunten, and R. J. Phillips, pp. 845–878, Univ. of Ariz. Press, Tucson, 1997.
Solomatov, V. S., Scaling of temperature- and stress-dependent viscosity convection, *Phys. Fluids*, *7*(2), 266–274, 1995.
Solomatov, V. S., Fluid dynamics of magma oceans, in *Origin of the Earth and Moon*, edited by R. Canup and K. Righter, pp. 323–328, Univ. of Ariz. Press, Tucson, 2000.
Solomatov, V. S., and L.-N. Moresi, Stagnant lid convection on Venus, *J. Geophys. Res.*, *101*(E2), 4737–4753, 1996.
Solomatov, V. S., and L.-N. Moresi, Three regimes of mantle convection with non-Newtonian viscosity and stagnant lid convection on the terrestrial planets, *Geophys. Res. Lett.*, *24*, 1907–1910, 1997.
Solomatov, V. S., and L.-N. Moresi, Scaling of time-dependent stagnant lid convection: Application to small-scale convection on Earth and other terrestrial planets, *J. Geophys. Res.*, *105*(B9), 21,795–21,818, 2000.
Solomatov, V. S., and L.-N. Moresi, Small-scale convection in the D layer, *J. Geophys. Res.*, *107*(B1), 2016, doi:10.1029/2000JB000063, 2002.
Solomatov, V. S., and D. J. Stevenson, Nonfractional crystallization of a terrestrial magma ocean, *J. Geophys. Res.*, *98*, 5391–5406, 1993.
Solomon, S. C., et al., Venus tectonics: An overview of Magellan observations, *J. Geophys. Res.*, *97*(E8), 13,199–13,255, 1992.
Solomon, S. C., M. A. Bullock, and D. H. Grinspoon, Climate change as a regulator of tectonics on Venus, *Science*, *286*(5437), 87–90, 1999.
Stofan, E. R., S. E. Smrekar, D. L. Bindschadler, and D. A. Senske, Large topographic rises on Venus: Implications for mantle upwelling, *J. Geophys. Res.*, *100*(E11), 23,317–23,328, 1995.
Strom, R. G., G. G. Schaber, and D. D. Dawson, The global resurfacing of Venus, *J. Geophys. Res.*, *99*(E5), 10,899–10,926, 1994.
Thompson, P. E., and P. J. Tackley, Generation of mega-plumes from the core-mantle boundary in a compressible mantle with temperature-dependent viscosity, *Geophys. Res. Lett.*, *25*, 1999–2002, 1998.
Turcotte, D. L., and G. Schubert, *Geodynamics*, 472 pp., Cambridge Univ. Press, New York, 2002.
van Keken, P. E., Evolution of starting mantle plumes: A comparison between laboratory and numerical models, *Earth Planet. Sci. Lett.*, *148*, 1–14, 1997.
Yuen, D. A., and W. R. Peltier, Mantle plumes and the thermal stability of the D" layer, *Geophys. Res. Lett.*, *7*, 625–628, 1980.
Zahnle, K., and K. McKinnon, Age of the surface of Venus (abstract), *Am. Astron. Soc. Bull.*, *28*, 1119, 1996.
Zhong, S., M. Gurnis, and L. Moresi, Free-surface formulation of mantle convection, 1, Basic theory and application to plumes, *Geophys. J. Int.*, *127*, 708–718, 1996.

A. T. Basilevsky, Vernadsky Institute of Geochemistry and Analytical Chemistry, Russian Academy of Sciences, Moscow, Russia.
J. W. Head, Department of Geological Sciences, Brown University, Providence, RI 02912, USA.
L.-N. Moresi, Department of Mathematics and Statistics, Monash University, Clayton, Victoria 3800, Australia.
A. V. Vezolainen and V. S. Solomatov, Department of Physics, New Mexico State University, Las Cruces, NM 88003, USA. (a_vez@nmsu.edu)